is not the case for the present system. It follows that the CO release observed in the present study must be due to a chemical process of low activation energy and complete reversibility at room temperature.

These observations prompt us to propose a new model, in which Pd carbonyl clusters interact with zeolite protons. It is known that bonds between H and Pd are strong; attaching a proton to a Pd_n cluster results in the formation of a positively charged $[H-Pd_n]^+$ cluster. CO ligands are less strongly bonded to such an electron-deficient cluster; some ligands, therefore, will be released while others remain attached to the cluster, but their characteristic IR frequency will shift to higher wavenumbers. The process can be written schematically:

$$Pd_n(CO)_a + H^+ \rightarrow [H-Pd_n(CO)_x]^+ + (a-x)CO_{gas}$$

This reaction may be either thermally neutral or slightly endothermic. Entropy drives it to the right under the conditions of Ar purging, but to the left when CO is admitted. Such reactions between cluster and cage wall will be typical for small clusters inside supercages in contrast to the behavior of large Pd particles. This model is supported by the observed intensity changes of the 3647-cm^{-1} band of the zeolite O-H bond. Also this process is completely reversible: when CO is reintroduced, the proton returns to the cage wall. The stretching frequency at 1823 cm^{-1} is typical for triply bonding CO on a neutral Pd_n cluster in state I. When the cluster acquires a positive charge by reacting with a proton, back-bonding from Pd to CO is diminished; it appears, therefore, possible that in state II the new band at 1860 cm^{-1}, which is separated from the eroding bands of state I by two sharp isosbestic points, represents the stretching frequency of the triply bonded CO on the electron-deficient cluster.

Zeolite protons may also interact with the oxygen atoms of CO ligands. This would result in changes of the stretching frequencies of both the zeolite O-H and the ligand C-O bonds, both being shifted toward lower wavenumbers. Indeed, a band shift in this direction is observed for the O-H band (in addition to the previously noted lower intensity), and one might speculate that the new shoulder in state II at 2060-2100 cm^{-1} is actually a red-shifted C-O stretching frequency of the terminal CO ligand. More work, however, will be necessary to substantiate this hypothesis.

Conclusions

Pd carbonyl clusters, apparently without precedent in the literature, are formed by admitting CO at room temperature to Pd/NaY, previously reduced at low temperatures, in which the size of the Pd clusters in the supercages is limited by the width of the cage windows. The IR spectrum, showing sharp bands, of the carbonyl cluster is quite different from spectra of adsorbed CO on supported transition metals. A cluster with 13 Pd atoms in its core could be consistent with the geometric constraints in faujasite supercages. The IR spectrum changes drastically upon purging at room temperature; new bands appear, separated by isosbestic points from the waning bands. The positions of the major IR bands are very similar to those reported for CO on Pd single crystals, which implies that also the heats of adsorption should be very similar. The easy release of CO from these clusters is, therefore, incompatible with thermal desorption; it is attributed to a reaction involving zeolite protons. IR data of the zeolite O-H band support this model.

Acknowledgment. Support from the U.S. Department of Energy under Contract DE-FG02-87ERA3654 is gratefully acknowledged.

Polarized Vacuum Ultraviolet Spectra of Crystalline Urea†

Blair F. Campbell‡ and Leigh B. Clark*

Contribution from the Department of Chemistry, University of California—San Diego, La Jolla, California 92093-0342. *Received May 1, 1989*

Abstract: Polarized vacuum UV reflection spectra from single crystals of urea and a urea-hydrocarbon adduct are reported. Corresponding absorption spectra are obtained through Kramers-Kronig analysis of the reflection data. Spectra taken from the (110) face of tetragonal urea show the presence of three strong absorption bands in the 56 000- to 65 000-cm^{-1} region. The results for urea are I (56 000 cm^{-1}, $f = 0.21$, B-type molecular excited-state symmetry, II (62 000 cm^{-1}, $f = 0.23$, A_1 symmetry), and III (65 000 cm^{-1}, $f = 0.09$, B-type symmetry). Reflection data and corresponding absorption spectra taken from the hexagonal urea-hexadecane adduct exhibit the same three transitions as found in urea, and in addition can be used to distinguish between $A_1 \rightarrow B_1$ and $A_1 \rightarrow B_2$ molecular transitions. The result is that both B-type excited states are of B_2 symmetry species. The effects of exciton mixing on the urea spectra are considered and found to be of minor importance. The experimental assignments differ significantly with the results from either of the two published theoretical calculations of the electronic spectrum of urea.

In spite of the historical fact that urea was the first laboratory synthesized organic molecule,[1] very little is known about its electronic spectrum. This lack is so despite its small-molecule nature (Figure 1), its relatively high symmetry (C_{2v}), and its candidacy as a fertile testing ground of theories aimed at understanding the electronic structure of the many important molecules made up of C, N, and O atoms. As far as we know, there have been published but two attempts at calculating the electronic spectrum of urea. The first calculation using a valence bond approach involving "interlocking amide resonance" was published by Rosa and Simpson[2] in 1964 and was followed by an ab initio calculation by Elbert and Davidson[3] in 1974. Experimental information is scant. Ley and Arends[4] reported a featureless onset of absorption in aqueous solution in the 180-185-nm range. An absorption spectrum of urea dissolved in trimethyl phosphate showing a single structureless absorption band centered at 58 800 cm^{-1} can be found in the doctoral dissertation of Rosa.[5] In addition, a spectrum of urea obtained by the SF_6 scavenger technique has been reported.[6]

†This work was supported by a National Institutes of Health grant (GM38575).

‡Present address: Rocketdyne Division, Rockwell International Corp., 6633 Canoga Ave., Canoga Park, CA 91303.

(1) Lipman, T. O. *J. Chem. Educ.* **1964**, *41*, 452.
(2) Rosa, E. J.; Simpson, W. T. In *Physical Processes in Radiation Biology*; Augenstein, L., Mason, R., Rosenberg, B., Eds.; Academic Press: New York, 1964; p 43.
(3) Elbert, S. T.; Davidson, E. R. *Int. J. Quantum. Chem.* **1974**, VIII, 857.
(4) Ley, H.; Arends, B. *Z. Phys. Chem.* **1932**, *B17*, 177.
(5) Rosa, E. J. Doctoral Dissertation, University of Washington, 1964.

0002-7863/89/1511-8131$01.50/0

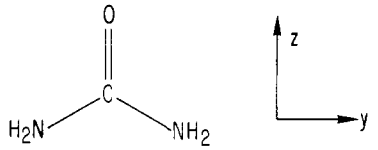

Figure 1. Structure of urea and molecular coordinate system.

Urea is closely related to the amide group, and this paper is an offshoot to another study of the electronic states of the amide group that is presently underway. Here we report polarized vacuum ultraviolet absorption spectra of single crystals of urea and of a urea–*n*-alkane clathrate or adduct crystal. The absorption curves are obtained from experimental reflection spectra through Kramers–Kronig analysis. Our aim is to identify the number of transitions, oscillator strengths, and excited-state symmetries for the urea molecule in the accessible wavelength range (to ~135 nm) so as to provide the kind of data that could direct and gauge theoretical calculations of such electronic systems.

Experimental Section

Urea (99+%) was purchased from Aldrich and was used without further purification. Crystals were grown from water solutions by slow evaporation. The crystals so obtained were thin plates elongated along *c* and showing (110) as the principal face. Crystal surfaces were not of high quality and exhibited a gravelly cast. However, perfect cleavage occurs along (110), and excellent surfaces were obtained thereby. The natural (gravelly) faces showed a general reduction of reflectivity of 20–25% relative to the cleaved surface. The identity of the (110) face was verified by X-ray methods.

Urea–hexadecane adduct crystals were kindly supplied by Professor R. R. Vold and had been grown by a very slow, controlled cooling procedure.[7] These crystals had been grown in 1984 and stored in a closed vial at room temperature since then. The hexagonal crystals had smooth, shiny surfaces and were elongated (~1 cm) along the *c* axis.

Solution spectra were measured in trimethyl phosphate (TMP) solvent (99+%, Aldrich). TMP from most suppliers contains absorbing impurities that limit its transparency in the vacuum UV. The Aldrich material, although exhibiting some absorption in the 250-nm region, is usable without further purification to 170.5 nm in our nitrogen-flushed Cary 15 using 0.10-mm commerical cells. The tetramethylurea was purchased from Aldrich.

The reflection spectrophotometer and Kramers–Kronig transformation procedures have been described before.[8] Instrumental modifications for the VUV have involved installation of choppers of different frequencies in the sample and reference beams so as to permit the extraction of the two signals with PAR 5209 lock-in amplifiers. A Hamamatsu R1460 photomultiplier (MgF_2 window) was used for detection, and a Hamamatsu L879 deuterium lamp (MgF_2 window) has replaced our old, noisy Hinterigger source.

Results

Urea. Urea crystallizes in the tetragonal $P\bar{4}2_1m$ system,[9,10] with two molecules per cell. The two C–O bonds in the unit cell lie exactly parallel to the *c* axis but in opposite directions to each other. The molecules are strictly planar and are rotated 90° around *c* with respect to each other. A projection of the unit cell onto (110) is given in Figure 2. The molecular plane at site 1 lies exactly perpendicular to (110), while that at site 2 is parallel to (110). The (110) face (as well as any other face parallel to the *c* axis) will provide two unique spectra. These two spectra arise from radiation polarized parallel and perpendicular to the *c* crystal axis and correspond to the allowed B_2 and E factor group states of the crystal, respectively.

The correlation between the symmetry species of the C_{2v} point group of the free urea molecule and the D_{2d} crystal factor group states is such that transitions to A_1 excited molecular states (*z* polarized) correlate with A_1 (forbidden) and A_2 (*c*-polarized) crystal states. The other two types of allowed, molecular transition, viz. to B_2 states (in-plane, *y*-polarized) and to B_1 states (out-of-plane, *x*-polarized), both correlate with degenerate E (⊥ to *c* polarized) crystal states. We thus expect that the full intensity (oscillator strength) of an $A_1 \rightarrow A_1$ transition will appear polarized along the *c* axis of (110), while one-half the intensity of both $A_1 \rightarrow B_1$ and $A_1 \rightarrow B_2$ transitions will appear polarized along the axis perpendicular to *c* of (110). Components of these bands will not appear along the opposite principal direction of the (110) face.

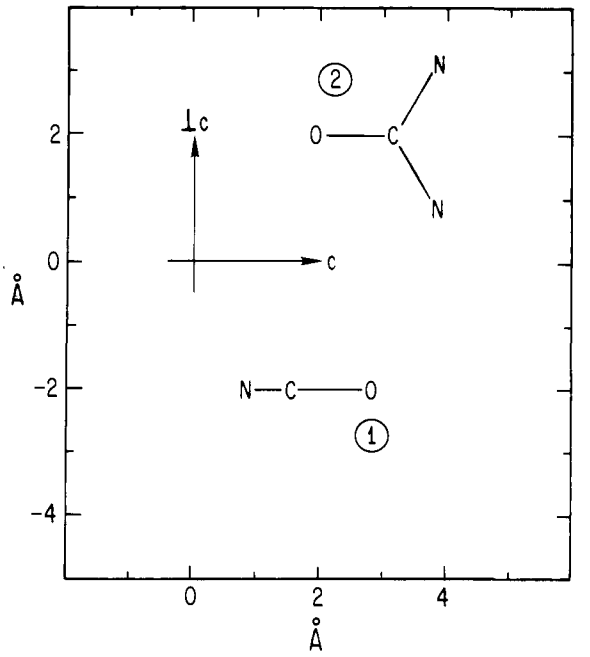

Figure 2. Projection of the two molecules of the unit cell onto the (110) plane. The site numbers are circled.

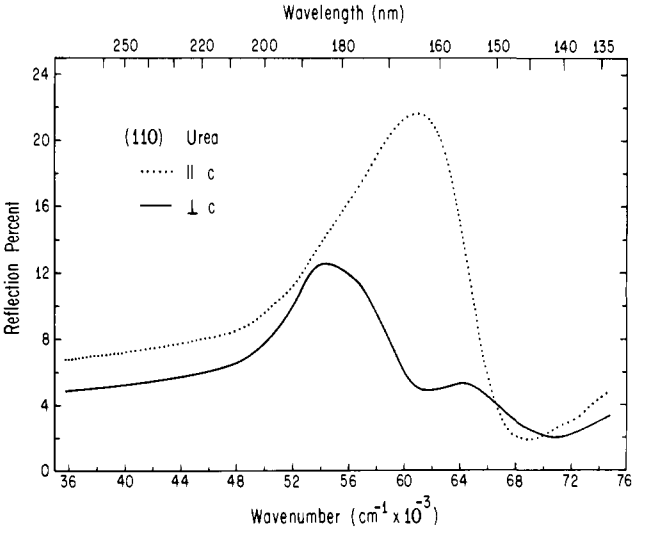

Figure 3. Reflection spectra for radiation incident on the (110) face of urea. The dotted and solid curves correspond to reflection polarized parallel and perpendicular, respectively, to the *c* crystallographic axis.

Reflection spectra taken from a freshly cleaved (110) face are shown in Figure 3. The Kramers–Kronig transformation procedure requires extrapolation of the measured reflection spectrum both to higher and lower frequency. These "trial" regions are then adjusted in a systematic way until the transformation produces essentially zero absorption throughout the known transparent region. The low-energy extrapolations were constructed by smoothly joining the measured reflection curves through the reflectivities calculated from known indices of refraction at 589 nm (N_0 = 1.484, R = 3.80%; N_E = 1.602, R = 5.35%).[11] The

(6) Naff, W. T.; Compton, R. N.; Cooper, C. D. *J. Chem. Phys.* **1973**, *57*, 1303.
(7) Greenfield, M. S.; Vold, R. L.; Vold, R. R. *J. Chem. Phys.* **1985**, *83*, 1440.
(8) Zaloudek, F.; Novros, J. S.; Clark, L. B., *J. Chem. Soc.* **1985**, *107*, 7344.
(9) Caron, A.; Donohue, J. *Acta Crystallogr.* **1964**, *17*, 544.
(10) Worsham, J. E.; Levy, H. A.; Peterson, S. W. *Acta Crystallogr.*, **1957**, *10*, 319.

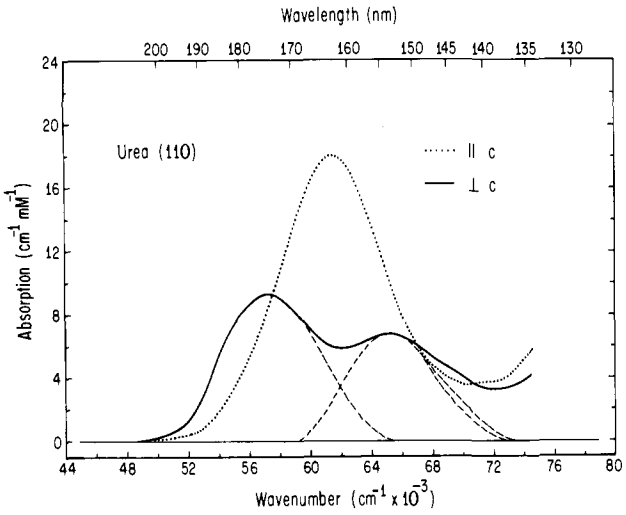

Figure 4. Absorption spectra for radiation polarized parallel (dotted) and perpendicular (solid) to the c axis of the (110) crystal face. These curves have been derived from the corresponding curves of Figure 3 by Kramers–Kronig analysis. Resolutions into separate band components are indicated as light dashed lines.

Table I. Spetral Data for (110) Urea

transition	$f_{\parallel c}$	$f_{\perp c}$	cm^{-1}	f_{iso}[a]	pol
I		0.31	56 000	0.21	x or y
II	0.65		62 000	0.23	z
III		0.13	65 000	0.09	x or y

[a] Isotropic oscillator strength $f_{iso} = (f_{\parallel c} + 2f_{\perp c})/3$.

corresponding absorption spectra are shown in Figure 4. Component oscillator strengths using the band resolutions shown in the figure were evaluated with the formula

$$f = 4.32 \times 10^{-9} \int \epsilon \, d\nu$$

where ϵ is the decadic molar extinction coefficient in $(cm \cdot M)^{-1}$ and ν is in wavenumbers (cm^{-1}) and are given in Table I. The strong band appearing along the c axis corresponds to an A_1 excited molecular state while the two distinct bands observed polarized perpendicular to c will have either B_1 or B_2 excited molecular symmetry. It is not possible to distinguish between these later two types from the urea data alone.

Urea–Hexadecane Adduct. The hexagonal structure (space group C_{6_12}) of this system is more complex. There are six urea molecules per primitive unit cell arranged such that adjacent cells develop channels parallel to the unique c axis along which straight-chain hydrocarbons can be positioned.[12] For the present crystal system (employing hexadecane) there is very nearly one hexadecane molecule for each two unit cells or for every 12 urea molecules. The relative spectroscopic dispositions or orientations of the six urea molecules of the unit cell are indicated on the projection shown in Figure 5. Note that neither is the hexadecane molecule shown nor is its channel obvious in this figure.

Examination of Figure 5 indicates that the C–O axis lies perpendicular to the c-crystal axis for all six molecules; however, only four sites yield an appreciable projection. A difference occurs in the projections of $y(A_1 \rightarrow B_2)$ and $x(A_1 \rightarrow B_1)$ polarized molecular transitions in that in-plane, y-polarized transitions will appear strongly along the c axis for all six molecules (with but a minor projection $\perp$ to c) while an x-polarized transition (i.e., $\perp$ to the molecular plane) will show the opposite behavior. It was this distinction between B_1 and B_2 states that made this system appealing for the clarification of the ambiguity found in urea. Site coordinates and direction cosines for the three principal molecular axes are given in Table II. From these direction cosines dichroic

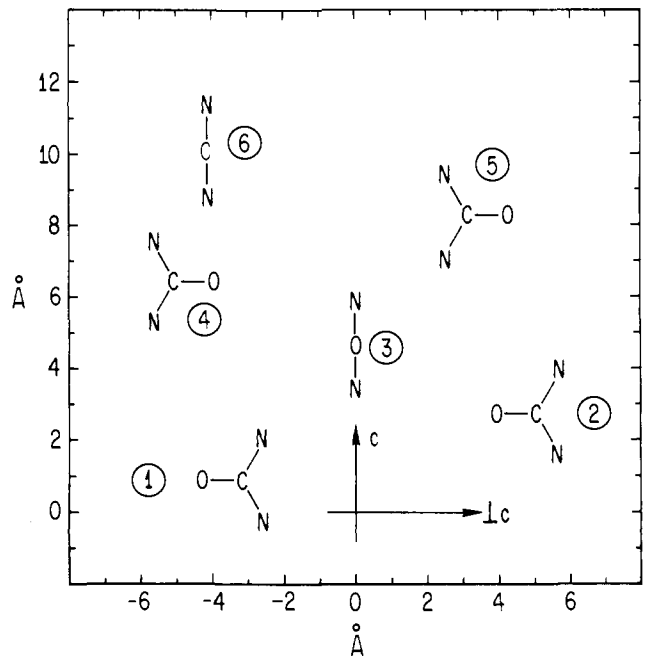

Figure 5. Projection of the six urea molecules of the urea–n-hexadecane adduct onto the face examined. The channel along which the hydrocarbon lies is parallel to c but is not obvious in this projection. The hydrocarbon chain is not shown. The six sites are labeled and correspond with the values in Table III. The individual C–O bonds of the molecules at sites 1, 2, 4, and 5 are canted by 30° in or out of the plane of the figure.

Table II. Carbon Atom Coordinates[a] and Direction Cosines of x, y, and z Axes of the Six Urea Sites of Urea–Hexadecane Adduct

site	pol	a	b	c
1		5.054	−2.9180	0.9205
	x	0.4959	0.8588	0.1285
	y	0.0642	0.1113	−0.9917
	z	−0.8660	0.5000	0
2		5.0540	2.9180	2.7625
	x	−0.4959	0.8588	0.1285
	y	−0.0642	0.1113	−0.9917
	z	−0.8660	−0.5000	0
3		0	5.8359	4.6045
	x	−0.9917	0	0.1284
	y	−0.1284	0	−0.9917
	z	0	−1.000	0
4		−5.054	2.9180	6.4455
	x	−0.4959	−0.8588	0.1285
	y	−0.0642	−0.1113	−0.9917
	z	0.8660	−0.5000	0
5		3.1760	−2.9180	8.2875
	x	0.4959	−0.8588	0.1285
	y	0.0642	−0.1113	−0.9917
	z	0.8660	0.5000	0
6		−4.1150	1.2915	10.1295
	x	0.9917	0	0.1284
	y	0.1284	0	−0.9917
	z	0	1.000	0

[a] Atom coordinates in Å for orthohexagonal unit cell.

ratios ($f_c/f_{\perp c}$) are calculated to be 0.034 and 120 for x- and y-polarized transition moments and clearly can distinguish transitions to B_1 and B_2 molecular excited states.

Reflection spectra for the a_0c_0 face are given in Figure 6 while the corresponding absorption curves obtained through Kramers–Kronig analysis are given in Figure 7. Although there is some latitude in resolving the bands into components, we feel the resolutions shown are reasonable and were used in evaluating the oscillator strengths given in Table III.

The correlation of the three transitions observed in neat urea crystals to the features observed in the adduct in straightforward. The first B-type urea transitions at 56 000 cm^{-1} appears now at

(11) Winchell, A. N. *The Optical Properties of Organic Compounds*; Academic Press: New York, 1954.
(12) Smith, A. E. *Acta Crystallogr.* **1952**, *5*, 224.

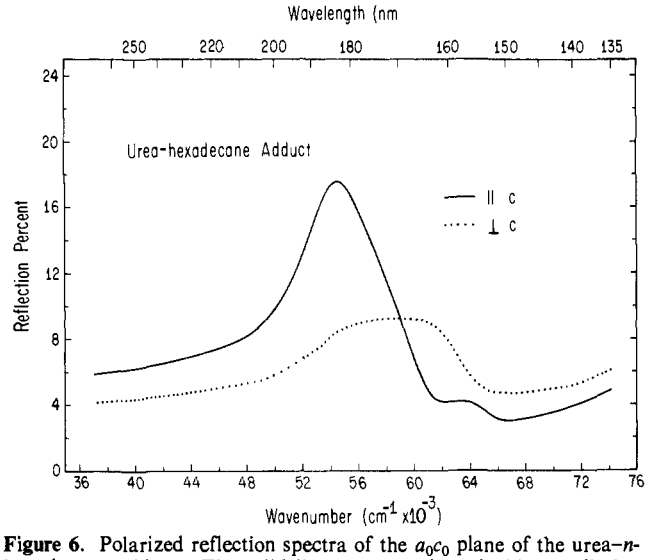

Figure 6. Polarized reflection spectra of the a_0c_0 plane of the urea–*n*-hexadecane adduct. The solid line corresponds to incident radiation polarized parallel to the c_0 crystallographic axis, while the dotted curve corresponds to radiation polarized perpendicularly to the c_0 axis.

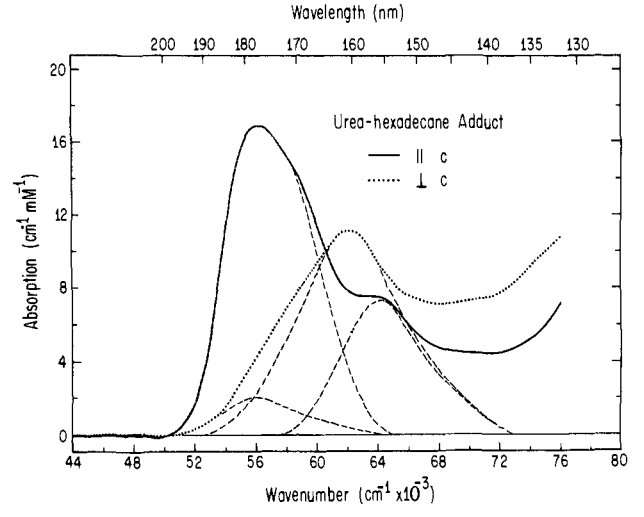

Figure 7. Polarized absorption spectra of the a_0c_0 plane derived by Kramers–Kronig analyses of the reflection spectra shown in Figure 5. The resolutions into components shown as light dashed lines were used in the evaluation of the oscillator strengths given in Table IV.

Table III. Comparison of Experimental Adduct Spectra to That Calculated Using the Urea Data

	f calcd from urea data		*f* obsd in adduct		
	a	*c*	*a*	*c*	assignment
I	0.005	0.61	0.05	0.53	$A_1 \rightarrow B_2$ (y)
II	0.34	0	0.46	?	$A_1 \rightarrow A_1$ (z)
III	0.02	0.26	?	0.22	$A_1 \rightarrow B_2$ (y)

[a] Assuming transition moment directions as given. [b] Using the resolutions shown in Figure 7.

56 200 cm^{-1} in the adduct along the *c* axis with about double the intensity as that observed in urea itself. This behavior is exactly that which is expected for a $A_1 \rightarrow B_2$ type transition. The second $A_1 \rightarrow B$ type transition of urea (65 000 cm^{-1}) appears at about 64 000 cm^{-1} in the adduct along the *c* axis with, again, about double the intensity as that observed in the urea crystals. We can therefore unequivocally assign both excited states to B_2 symmetry species. The lone $A_1 \rightarrow A_1$ transition found at 61 800 cm^{-1} in the adduct appears with about half the intensity found for urea and is polarized along the $\perp c$ direction of the adduct. Again this behavior is what is predicted for such a transition moment.

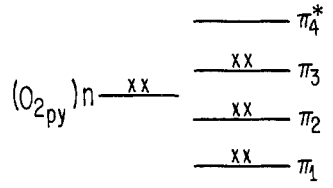

Figure 8. Schematic orbital energy level diagram for urea.

A comparison of the observed oscillator strengths of the adduct to those expected based on the neat urea data using the oriented gas model is given in Table III. We feel that the close matchup in this regard confirms the assignments of all three bands, and so our results can be summarized as follows: $A_1 \rightarrow B_2$ (56 000 cm^{-1}, $f = 0.21$), $A_1 \rightarrow A_1$ (62 000 cm^{-1}, $f = 0.23$), and $A_1 \rightarrow B_2$ (65 000 cm^{-1}, $f = 0.09$). The oscillator strengths here have been randomized and therefore would represent isotropic (solution spectrum) values.

Discussion

The NV Transitions. A basis for assigning the observed transitions is shown in Figure 8 where the six π electrons are shown schematically. Here, n is a nonbonding O_{2p_y} orbital. The transition $n \rightarrow \pi^*_4$ (where π^*_4 is predominantly the antibonding carbonyl π^* orbital) is forbidden and may occur weakly owing to vibronic distortions. The three remaining occupied π orbitals are basically the bonding and antibonding combinations of the N_{2p_π} orbitals and the carbonyl π(CO). Other possible valence shell orbitals will be σ or σ^* in nature. The original work by Rosa and Simpson[2] led to the lowest excited state as being of A_1 symmetry and therefore reached through z(C–O) polarization. They assigned the broad absorption band that they observed in trimethyl phosphate solution at 58 800 cm^{-1} to this transition. Their valence bond formulation led to no other excited configurations although the presence of the weak $n \rightarrow \pi^*_4$ was presumed buried beneath the stronger absorption.

The Gaussian orbital, ab initio calculation by Elbert and Davidson[3] led to a totally different assignment. Their calculation made the lowest energy singlet transition out to be $n \rightarrow \pi^*_4$ at 57 600 cm^{-1}. The first $\pi \rightarrow \pi^*$ band was then predicted to occur at ~73 000 cm^{-1}. Since the absorption observed experimentally by Rosa fell close to their predicted $n \rightarrow \pi^*_4$ transition energy, they reassigned this band as $n \rightarrow \pi^*_4$. This assignment was made in spite of the fact that such a transition ought to be of low absorption strength, whereas Rosa had estimated the molar extinction coefficient to be about 10 000 $(cm \cdot M)^{-1}$.[5]

The situation in this regard has been summarized by Robin[13] who pointed out that the ab initio calculation was not done with the benefit of expanded Gaussian orbitals, so that a shift to lower energy of some 10 000 cm^{-1} might be expected for the $\pi \rightarrow \pi^*$ bands relative to the published values. Robin concludes by noting that urea is isoelectronic with carbonate ion in which the π_2 and π_3 orbitals are degenerate. In urea the degeneracy will be broken so that the two transitions ($\pi_2 \rightarrow \pi^*_4$, $\pi_3 \rightarrow \pi^*_4$) may be split by ~6000 cm^{-1} and lie close to the amide transition energy (56 000 cm^{-1}).[14] Robin's inferences seem well grounded, for the two lowest energy bands do have nearly equal intensities, are separated by ~5000 cm^{-1}, and occur in the vicinity of the amide NV_1 transition (56 000 cm^{-1}). Finally, we note that the published spectra of crystalline calcite ($CaCO_3$) show a strong, degenerate (in-plane polarized) transition at 64 000 cm^{-1}.[15]

The origin of the second B_2 excited state (65 000 cm^{-1}) must lie outside the π electron manifold, for there is but one $A_1 \rightarrow B_2$ transition among all possible connections of π_1 through π^*_4. If it originates from the nonbonded oxygen electron pair, then the

(13) Robin, M. B. *Higher Excited States of Polyatomic Molecules*; Academic Press: Orlando, FL, 1985; Vol. III.
(14) Robin, M. B. *Higher Excited States of Polyatomic Molecules*; Academic Press:. New York, 1975; Vol. II.
(15) Kondo, S.; Yamashita, H., Nakamura, K. *J. Phys. Soc. Jpn.* **1973**, *34*, 711.

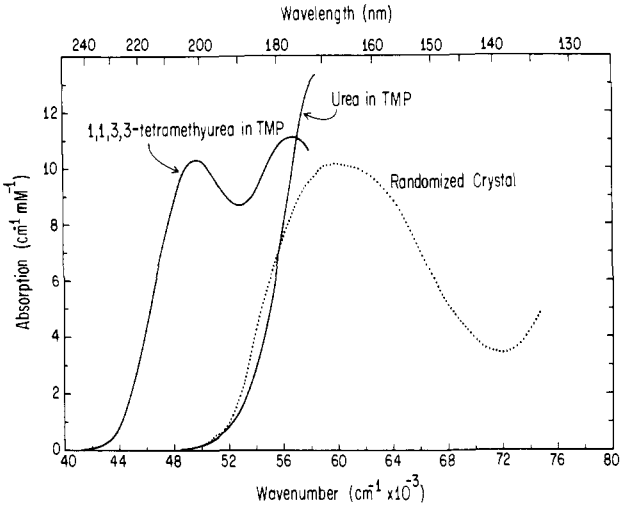

Figure 9. Solution spectra of 1,1,3,3-tetramethylurea and urea in trimethyl phosphate (TMP) solvent. The dotted curve corresponds to a randomized urea crystal spectrum, and was obtained by multiplying the $\perp c$ spectrum of (110) by 2, adding the $\| c$ spectrum of (110), and dividing by 3.

excited state must be of A_1 symmetry involving a σ^* orbital. Although a Rydberg assignment can probably be ruled out in the condensed phase, the assignment of this third valence shell transition remains obscure.

$n\pi^*_4$ Transition. We have examined the low-energy region leading up to the first strong absorption band of urea and have found no hint of a weak band that could be assigned as the $n \rightarrow \pi^*_4$ transition. Polarized absorption measurements through a ~1-mm thick crystal slab show simple absorption edges that are consistent with no "extraneous" weak absorption in the low-energy region. These absorption edges (OD = 0.5) occur at 211 nm and 208 nm for radiation polarized $\perp c$ and $\| c$, respectively. Since urea is 22.0 M in the neat crystal, these wavelengths correspond to molar extinction values of about 0.2 ($cm \cdot M^{-1}$). We conclude that the $n\pi^*_4$ transition must be at shorter wavelengths yet and so lies buried beneath the strong NV bands. There does occur a broad peak at 48 800 cm^{-1} (205 nm) in the SF_6 scavenger spectrum reported by Naff and Compton;[6] however, it is not clear that this peak is related to any transition in the optical spectrum of urea.

Solution Spectra. We have measured the spectrum of urea in trimethyl phosphate solvent and compared it to that reported by Rosa.[5] We believe that the absorption contour and peak position given by Rosa is distorted owing to the onset of solvent absorption. This onset of absorption of the TMP solvent itself is sudden and rapid at about 172 nm (58 000 cm^{-1}). Rosa's single beam technique employing a demountable cell is subject to large distortions and false maxima in the vicinity of the solvent absorption edge. The double-beaming, double-dispersing instrument (Cary 15) used here is not subject to these problems. Robin[14] has reported (unpublished) that the vapor spectrum of 1,1,3,3-tetramethylurea shows strong bands at 48 100, 58 800, and 76 000 cm^{-1}. The lowest two apparently correspond to the bands observed at 49 600 cm^{-1} and 56 700 cm^{-1} for this compound dissolved in trimethyl phosphate (Figure 9). If these transitions correspond to the first two bands found in crystalline urea, then red shifts of some 8000 cm^{-1} and 2000 cm^{-1} have occurred. Since methylation at the nitrogen atoms ought to effect a transition strongly localized in the N–C–N region more than say the $\pi \rightarrow \pi^*$ transition of the carbonyl, the large red shift of the first $A_1 \rightarrow B_2$ transition is consistent with our general analysis for the lowest energy NV transition as involving an electron from the antibonding combination of the nitrogen $2p_\pi$ orbitals. Unfortunately, trimethyl phosphate is not transparent deep enough into the vacuum UV so as to be able to characterize the third valence shell band. The solution spectra are shown in Figure 9 together with a "randomized" urea crystal spectrum obtained by doubling the $\perp c$ spectrum, adding the $\| c$ spectrum, and then dividing by 3. There appear to be no surprizes in any of the solution data.

Table IV. Dipole–Dipole Lattice Sums for $\hat{\mathbf{k}} \perp$ to (110) of Urea (in $cm^{-1}/Å^2$)[a-c]

sites	*zz*	*yy*	*xx*	*zy*	*zx*	*yx*
1,1	−5166	7415	−2250	0	0	0
2,2	−5166	−2250	7415	0	0	0
1,2	956	0	0	0	0	5310
2,1	956	0	0	0	0	−4335

[a] Molecule at site 2 is generated by a C_4 rotation about *c* followed by a reflection in the plane $\perp c$. [b] Dipole centers were taken at the C atom. Site 1: (0, 0.5000, 0.3308) as fractional unit cell coordinates. [c] *x*, *y*, *z* dipole polarization direction are as in Figure 1.

Table V. Model Spectrum for the Urea Molecule

	cm^{-1}	f_{iso}[a]	**d** (Å)[b]	pol
I	56 800	0.205	0.588	*y*
II	63 400	0.227	0.585	*z*
III	65 300	0.088	0.357	*y*

[a] Isotropic oscillator strength. [b] Dipole transition moment length.

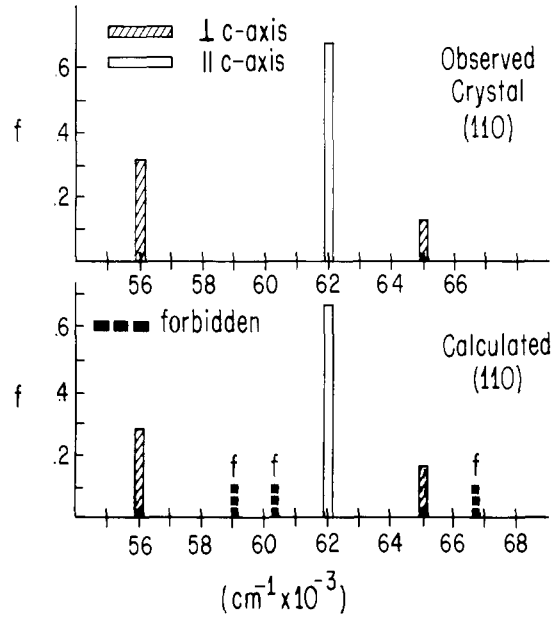

Figure 10. Comparison of the observed urea (110) crystal spectra to that calculated from the model urea spectrum given in Table V with the point dipole approximation.

Crystal Interactions. Crystal interactions commonly result in crystal state mixing that lead to deviations in energies, oscillator strengths, and dichroic ratios from that predicted with the oriented gas model. The high symmetry and tetragonal nature of the urea system, however, minimize these types of complications. Nevertheless, we have carried through an exciton mixing calculation in the dipole approximation to assess the effects of the crystal field. For the (110) face of urea the two molecules of the unit cell are not spectroscopically equivalent, and the Hamiltonian matrix cannot be factored by symmetry. The secular determinant is therefore of dimension six (i.e., 2 sites × 3 transitions). Matrix elements can be evaluated in terms of lattice sums in which the intermolecular interaction part is formally equivalent to lattice sums of dipole–dipole interactions. The necessary sums evaluated with the Ewald–Kornfeld procedure for wave vector, $\hat{\mathbf{k}}$, perpendicular to (110) in the limit $|\mathbf{k}| \rightarrow 0$ are given in Table IV for unit vectors (1 Å) directed along the molecular *x*, *y*, and *z* axes.[16,17]

One must choose a model spectrum for the free urea molecule as a basis for the crystal calculation. The model urea spectrum that provides a close fit to the observed crystal spectra is as given

(16) Fox, D.; Yatsiv, S. *Phys. Rev.* **1957**, *108*, 938.
(17) Kornfeld, H. *Z. Phys.* **1924**, *22*, 27.

in Table V. The results of a calculation using this model spectrum are displayed graphically in Figure 10. Each free molecule transition generates one allowed and one forbidden crystal state. No mixing occurs between the $A_1 \rightarrow A_1$ and $A_1 \rightarrow B_2$ transitions; however, modest mixing occurs between the two $A_1 \rightarrow B_2$ transitions. The result here is to shift ~10% of the intensity of I into III. The crystal field effects are therefore of little consequence in the basic interpretation of the crystal spectra and the assignments of the transitions.

Adduct-Hydrocarbon Spectrum. No absorption that is attributable to the hexadecane molecule in the urea adduct spectra can be definitely discerned. Based on the neat urea data, there is about 35% "extra" absorption over that expected in the vicinity of 60000 cm^{-1} for the $\|c$ spectrum of the adduct, and this intensity could conceivably arise from transitions based on the hydrocarbon. The molar concentration of the hydrocarbon in the adduct crystal is 1.3 mol/L compared to a value of 15.4 for the urea presence. We then estimate that if the extra intensity is attributable to the hydrocarbon, then the molar extinction coefficient for hexadecane would have a magnitude ~2000 cm^{-1} M^{-1}, and its polarization would be transverse to the hydrocarbon long axis. In fact, absorption of long *n*-alkanes begins at about 60000 cm^{-1} and rises more or less continuously toward higher energy.[18] A positive identification, however, is not possible here. We thank Professor B. Hudson (University of Oregon) for alerting us to this interesting type of crystal system.

Summary

Polarized reflection spectra from single crystals of urea and urea-hexadecane adduct have been used to identify the excited-state symmetries of three valence shell transitions in the vacuum ultraviolet. The results from an oriented gas analysis of the data unambiguously give the three transitions as I (56000 cm^{-1}, f = 0.21, $A_1 \rightarrow B_2$), II (62000 cm^{-1}, f = 0.23, $A_1 \rightarrow A_1$), and III (65000 cm^{-1}, f = 0.09, $A_1 \rightarrow B_2$). Crystal field induced shifts and mixing are of minor significance in urea. The observed urea crystal spectra can be closely fit by a model spectrum with but minor energy shifts (+800, +1400, +300 cm^{-1} for I, II, and III) from those given above. The lowest energy $A_1 \rightarrow B_2$ transition is assigned as an electron transition between predominantly the antibonding combination of $2p_\pi$ nitrogen orbitals and π^* of the carbonyl, while the $A_1 \rightarrow A_1$ transition must be essentially the $\pi \rightarrow \pi^*$ of the carbonyl. No assignment of the third observed band ($A_1 \rightarrow B_2$) can be made.

(18) Raymonda, J.; Simpson, W. T. *J. Chem. Phys.* **1967**, *47*, 430.

On the Mechanism of $SnCl_4$-Promoted Additions of Allylstannanes to Aldehydes: A Response to Denmark, Wilson, and Willson

Gary E. Keck,* Merritt B. Andrus, and Stephen Castellino†

Contribution from the Department of Chemistry, University of Utah, Salt Lake City, Utah 84112. *Received November 2, 1987*

Abstract: The reaction of allyltri-*n*-butylstannane with the complexes formed from three aldehydes (**1-3**) with $SnCl_4$ has been investigated via variable-temperature ^{119}Sn NMR spectroscopy under carefully controlled conditions. With aldehyde **1**, which forms a tight bidentate chelate with $SnCl_4$, addition products are produced without the intermediacy of the transmetalation product allyltrichlorostannane at 1:1 stoichiometry, as revealed by appropriate control experiments with this reagent. The same is true of 2:1 (aldehyde:$SnCl_4$) complexes derived from **1** and **2** provided that such complexes are formed stoichiometrically at low temperature and free $SnCl_4$ is not present. With **3**, free $SnCl_4$, chelate, and 2:1 complex are all in equilibrium at -80 to -90 °C at 1:1 $SnCl_4$:aldehyde stoichiometry, and transmetalation with free $SnCl_4$ is an important component of the overall reaction pathway. Competition experiments between the chelate and the 2:1 complex derived from **1** reveal that the chelate is more reactive but that the rate difference is modest. In addition, a mechanistic/spectroscopic study of allylstannane additions to aldehydes reported recently by Denmark, Wilson, and Willson has been reinvestigated, and results contrary to those reported are presented. In particular, it is shown that transmetalation pathways involving conversion of allyltri-*n*-butylstannane to allyltrichlorostannane or diallyldichlorostannane prior to reaction with aldehydes **5** and **6** do not occur from stable 2:1 $(RCHO)_2 \cdot SnCl_4$ complexes at low temperature. The sensitivity of such experiments to experimental details is emphasized.

Previous studies in our laboratories[1] have revealed that the preferred solution structures of complexes derived from β-alkoxy aldehydes and various Lewis acids (e.g., $MgBr_2$ and $TiCl_4$) are an extremely sensitive function of aldehyde structure and that the most complex behavior is observed with $SnCl_4$. This case provides an opportunity to assess the mechanistic consequences of such structural variations in allylstannane addition reactions, particularly issues involving transmetalation reactions,[2] which are relevant both to synthetic applications and to other mechanistic investigations.[3] We record herein the results of a study of the dynamics of such reactions as revealed by ^{119}Sn NMR.[4,5]

Shown in Figure 1 are selected data points for the reaction of allyltri-*n*-butylstannane with the bidentate chelate formed from the β-benzyloxy aldehyde **1** and $SnCl_4$, as observed by ^{119}Sn NMR at -90 °C. The resonances for the chelate at -577 ppm and

†Department of Chemistry, North Dakota State University, Fargo, ND 58102.

(1) (a) Keck, G. E.; Castellino, S. *J. Am. Chem. Soc.* **1986**, *108*, 3847. (b) Keck, G. E.; Castellino, S.; Wiley, M. R. *J. Org. Chem.* **1986**, *51*, 5478. (c) Keck, G. E.; Castellino, S. *Tetrahedron Lett.* **1987**, *28*, 281. (d) Keck, G. E.; Castellino, S., unpublished results.

(2) (a) Tagliavini, G.; Peruzzo, V.; Plazzogna, G.; Marton, D. *Inorg. Chem. Acta* **1977**, *24*, L47. (b) Peruzzo, V.; Tagliavini, G. *J. Organomet. Chem.* **1978**, *162*, 37. Gambaro, A.; Marton, D.; Tagliavini, G. *Ibid.* **1981**, *210*, 57. (c) Gambaro, A.; Marton, D.; Peruzzo, V.; Tagliavini, G. *Ibid.* **1982**, *226*, 149. (d) Gambaro, A.; Boaretto, A.; Marton, D.; Tagliavini, G. *Ibid.* **1983**, *231*, 307. (e) Tagliavini, G. *Rev. Silicon, Germanium, Tin, Lead Cmpds.* **1985**, *8*, 237. (f) Fishwick, M. W.; Wallridge, M. G. H. *J. Organomet. Chem.* **1977**, *136*, C46. (g) Yamamoto, Y.; Maeda, N.; Maruyama, K. *J. Chem. Soc., Chem. Commun.* **1983**, 742. (h) Keck, G. E.; Abbott, D. E.; Boden, E. P.; Enholm, E. J. *Tetrahedron Lett.* **1984**, *25*, 3927. (i) Denmark, S. E.; Wilson, T.; Willson, T. M. *J. Am. Chem. Soc.* **1988**, *110*, 984.

0002-7863/89/1511-8136$01.50/0